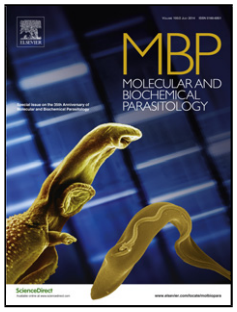

Title: Anti-trypanosomal activity of cationic *N*-heterocyclic carbene gold(I) complexes

Authors: Isabel Winter, Julia Lockhauserbäumer, Gertrud Lallinger-Kube, Rainer Schobert, Klaus Ersfeld, Bernhard Biersack

PII: S0166-6851(17)30055-5
DOI: http://dx.doi.org/doi:10.1016/j.molbiopara.2017.05.001
Reference: MOLBIO 11069

To appear in: *Molecular & Biochemical Parasitology*

Received date: 4-11-2016
Revised date: 4-5-2017
Accepted date: 12-5-2017

Please cite this article as: Winter Isabel, Lockhauserbäumer Julia, Lallinger-Kube Gertrud, Schobert Rainer, Ersfeld Klaus, Biersack Bernhard.Anti-trypanosomal activity of cationic N-heterocyclic carbene gold(I) complexes.*Molecular and Biochemical Parasitology* http://dx.doi.org/10.1016/j.molbiopara.2017.05.001

Anti-trypanosomal activity of cationic *N*-heterocyclic carbene gold(I) complexes

Isabel Winter [a], Julia Lockhauserbäumer [a], Gertrud Lallinger-Kube [a], Rainer Schobert [b], Klaus Ersfeld [a,*], Bernhard Biersack [b,*]

[a] *Laboratory of Molecular Parasitology, Department of Genetics, University of Bayreuth, 95440 Bayreuth, Germany*

[b] *Organic Chemistry Laboratory, University of Bayreuth, 95440 Bayreuth, Germany*

[*]Corresponding authors. Phone: +49(0)921 552673 (BB); +49(0)921 552710 (KE). Fax: +49(0)921 552671 (BB); +49(0)921 552726 (KE).

E-mail: bernhard.biersack@yahoo.com; klaus.ersfeld@uni-bayreuth.de.

Graphical abstract

Highlights

- Gold(I) complexes **1a** and **1b** showed excellent in vitro activity against *T. b. brucei*.
- **1a** and **1b** quickly destroyed the cytoskeleton of *T. b. brucei* cells at low doses.
- Reduced toxicity towards human HeLa cells was observed for **1a** and **1b**.

Abstract

Two gold(I) *N*-heterocyclic carbene complexes **1a** and **1b** were tested for their anti-trypanosomal activity against *Trypanosoma brucei brucei* parasites. Both gold

compounds exhibited excellent anti-trypanosomal activity (IC_{50} = 0.9-3.0 nM). The effects of the gold complexes **1a** and **1b** on the *T. b. brucei* cytoskeleton were evaluated. Rapid detachment of the flagellum from the cell body occurred after treatment with the gold complexes. In addition, a quick and complete degeneration of the parasitic cytoskeleton was induced by the gold complexes, only the microtubules of the detached flagellum remained intact. Both gold compounds **1a** and **1b** feature selective anti-trypanosomal agents and were distinctly more active against *T. b. brucei* cells than against human HeLa cells. Thus, the gold complexes **1a** and **1b** feature promising drug candidates for the treatment of trypanosome infections such as sleeping sickness (human African Trypanosomiasis caused by *Trypanosoma brucei* parasites).

Abbreviations: AB assay, Alamar Blue assay; BBB, blood-brain-barrier; HAT, human African Trypanosomiasis; NHC, *N*-heterocyclic carbene; NTD, neglected tropical diseases.

Keywords: Gold; NHC complexes; Organometallics; Anti-parasitic drugs; Cytoskeleton; Trypanosomes.

1. Introduction

Trypanosomes of the species *Trypanosoma brucei* are parasitic eukaryotes of the African continent [1]. *T. brucei* parasites can cause severe diseases both in humans and in animals [2-5]. Human pathogenic *T. brucei* parasites cause human African Trypanosomiasis (HAT) or sleeping sickness, a lethal disease for humans (unless treated with anti-parasitic drugs) that belongs to the class of neglected tropical diseases

(NTD) [6,7]. *T. brucei* parasites undergo a complex life cycle in the vector (tsetse fly) and the mammalian host with various developmental forms, i.e., trypomastigotes (metacyclic and procyclic) and epimastigotes in the tsetse fly, and ´´slender´´ and ´´stumpy´´ trypomastigotes in the host blood and lymph [8-10]. There are only a few approved drugs available for the treatment of HAT [7,11]. These drugs are often expensive and/or possess grave side effects [3,12,13]. Hemolymphatic stages of *T. brucei* infections are treated with suramin and pentamidine. Advanced neurologic stages require crossing of the blood-brain-barrier (BBB) by the drug molecules and, in particular, advanced *T. b. rhodesiense* infections are treated with melarsoprol, an arsenic compound that is highly toxic [11-13]. The BBB-crossing drugs nifurtimox and eflornithine are further drugs suitable for the treatment of advanced stages of *T. b. gambiense* only [14]. Innovative screening methods have led to the orally applicable anti-trypanosomal drugs fexinidazole (nitroimidazole derivative, in phase III clinical trials) and SCYX-7158 (oxaborole derivative, in phase I clinical trials) [15].

The cytoskeleton of trypanosomes is dominated by an array of sub-pellicular microtubules and the axoneme of the flagellum. It is essential for morphology, organelle positioning, cell division and motility. Thus, the *T. brucei* cytoskeleton can be a suitable target for new anti-trypanosomal drugs. Tubulin binders like trifluralin, colchicine and vinblastine displayed potent activity against trypanosomes, but are not sufficiently selective for tubulin of the parasite [16,17]. However, progress has been made to identify highly selective tubulin inhibitors in trypanosomes [18]. Microtubule-associated kinesins feature further suitable protein targets [19-21].

Gold has been applied for medicinal purposes since ancient times and the application of gold compounds in modern medicine started with the discovery of the anti-tuberculosis activity of gold compounds in the 19th century [22]. Meanwhile, gold complexes such as auranofin are widely applied in modern medicine for the treatment of

rheumatoid arthritis [23]. In addition, gold complexes have raised interest as possible anticancer agents [24]. The anti-parasitic activities of several gold complexes were also reviewed [25]. The gold complex auranofin inhibits trypanothione by a dual mechanism involving the gold and the sugar component of the auranofin molecule [26]. Metal-NHC (*N*-heterocyclic carbene) complexes are of high importance as catalysts for organic reactions, but meanwhile gold-NHC complexes have also revealed distinct biological activity such as anticancer activity [24]. Recently, Gornitzka and coworkers have disclosed a gold-NHC complex with high anti-plasmodial activity [27]. In addition, iridium and rhodium NHC complexes have shown promising trypanocidal activities [28]. The biological potential of ferrocenes as bioactive phenyl surrogates and bioisosteres has been reviewed thoroughly [29-31]. Enhanced tumor selectivity of the non-discriminating fungal cytotoxin illudin M by esterification with ferrocene-1,1'-dicarboxylate was observed [32-34]. In addition, ferrocene derivatives were able to overcome multidrug resistance in cancer cells that overexpress the Pgp transporter [35-37]. Concerning pathological bugs and parasites, ferrocene-modified aminohydroxynaphthoquinones derived from lawsone exhibited parasite growth inhibitory activity against *Toxoplasma gondii* [38]. Ferroquine, a ferrocene derivative of chloroquine, is a potent antimalarial compound [39]. Recently, a series of ferrocene-modified benzyl diamines showed distinct anti-parasitic activity against *T. brucei* and *T. cruzi* parasites [40].

Herein, we investigated the anti-trypanosomal activity of the cationic gold(I) NHC complex **1a** and its ferrocene derivative **1b** (Fig. 1). Both of them have shown strong cytoskeleton damages in aggressive cancer cells [41,42] and, therefore, the effects of these gold complexes on the trypanosomal cytoskeleton were also evaluated.

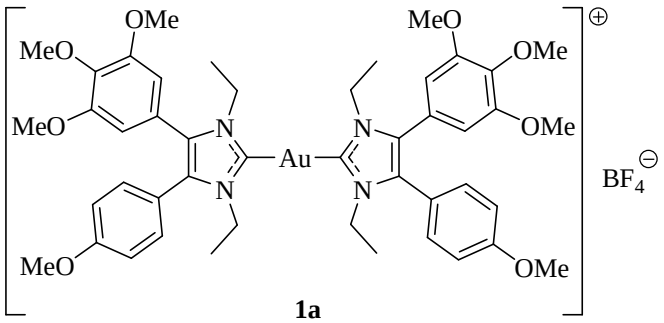

1a

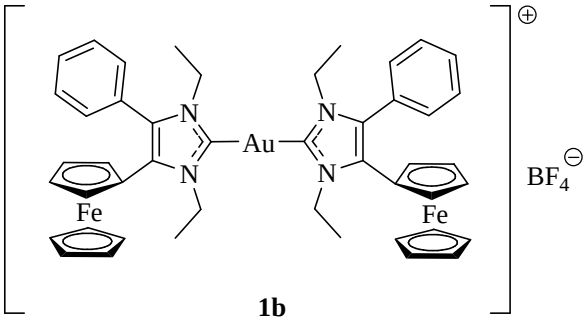

1b

Fig. 1. Chemical structures of the gold(I) bis-carbene complexes **1a** and **1b**.

((single column fitting image))

2. Material and methods

2.1. Biological studies

2.2.1. Cell lines and culture conditions

Cells of the *T. b. brucei* bloodstream-form cell line S16, a derivative of *T. b. brucei* strain Lister 427 [43], were maintained in HMI-9 medium, pH 7.5, supplemented with 10% fetal bovine serum (FBS) in a humidified 5% CO_2 atmosphere at 37 °C. The human HeLa cells were grown in DMEM medium (DMEM High Glucose with L-glutamine without sodium pyruvate, Biowest) supplemented with 10% FBS, 1% streptomycin and penicillin in a humidified 5% CO_2 atmosphere at 37 °C.

2.2.2. Alamar Blue (AB) assay

The AB assay was used to identify viable cells after treatment with drug candidates [44-47]. This assay is based on the irreversible reaction of the blue dye resazurin and NADH to pink resofurin in intact cells. *T. b. brucei* cells (8×10^3/well) were seeded on 96-well microplates, treated with the test compounds (dissolved in DMSO) and incubated for 72 h (5% CO_2, 95% humidity, 37 °C). 10 µL of the AB reagent (500 µM resazurin sodium salt in PBS) was added and incubated for further 4-8 h at 37 °C. The fluorescence (extinction at 544 nm, emission at 590 nm) was measured on an Omega Fluostar (BMG Labtech) fluorescence plate reader. HeLa cells (1300/well) were seeded on 96-well microplates, and after 24 h (for attachment to the surface) the HeLa cells were treated in the same way as the trypanosomes.

2.2.3. Immunofluorescence staining of HeLa cells and trypanosomes

The DMEM medium was removed from HeLa cell cultures and the cells were washed with PBS. Trypsin-EDTA (1 mL) was added and the cells were incubated for 2 min at 37 °C. The cells were re-suspended in DMEM medium (9 mL) and centrifuged for 2 min at 1250 x g. The supernatant was discarded and the cell pellet suspended in DMEM medium (9 mL). 0.5 mL of the cell suspension was added to each well (containing 1.5 mL DMEM) of a 12-well plate at 37 °C (total volume in each well = 2 mL), then a round glass coverslip (diameter of 18 mm) pre-treated with 70% ethanol was laid into the wells, and the cultures were incubated for 12-24 h at 37 °C and 5% CO_2 in order to achieve cell attachment to the coverslip. Then, the cells were treated with the test compounds (1 µM, 10 µM) and incubated for 1 h, 3 h, 6 h, or 9 h at 37 °C and 5% CO_2. The coverslips with the attached cells were transferred into another 12-well plate containing PBS. After washing with PBS for three times, PBS was removed from the wells and the HeLa cells were fixed by treatment with ice-cold methanol for 1 h at 4 °C. The methanol was removed and the cells were washed again for three times with PBS. Primary antibody (mouse monoclonal anti α-tubulin antibody, TAT, 1 µg/mL

in PBS, 150-200 µL) was added to the cells and incubated at room temperature in a humid chamber for 1 h. The coverslips were washed with PBS for three times and secondary antibody (Anti-Mouse IgG ATTO 550, Sigma, 1.5 µg/mL in PBS) was added to the cells and incubated in a humid chamber in the dark at room temperature for 1 h. After washing with PBS for three times (5 minutes) and discarding of the PBS, the cells were embedded with 5 µL Vectashield Mounting Medium containing DAPI (Vector Laboratories) and analysed by fluorescence microscopy.

Similarly, trypanosome cells ($3x10^6$ cells/mL) were placed into 12-well plates containing supplemented HMI-9 medium (1 mL) at 37 °C. Test compounds (0.1 µM, 0.5 µM, 1 µM, 10 µM) were added and the cells were incubated for 0.5 h, 1 h, 3 h, and 6 h at 37 °C and 5% CO_2. After centrifugation at 3000 x g for 5 min, the cell pellet was resuspended in 500 µL PEME medium (0.1 M PIPES, 2 mM EGTA, 1 mM $MgSO_4$, 0.1 mM EDTA, pH 6.9) and washed with PEME for three times. The cells (150 µL, in PEME buffer) were placed on poly-lysine-coated glass microscope slides and incubated to attach to the slide in a humid chamber for 10 min at room temperature. After careful washing with PEME and incubation with ice-cold 1% NP40 in PEME for 5 min, the cells were briefly washed in PEME and then fixed in ice-cold methanol for 1 h followed by treatment of the fixed cells with PBS for 5 min. Staining with the primary and secondary antibodies and processing for fluorescence analysis were carried out accordingly to the HeLa cell protocol described above.

For the DAPI-DIC experiments in the absence of NP40, trypanosome cells ($3x10^6$ cells/mL) were placed into 6-well plates. Test compounds were added (1 µM) und the cells were incubated for 0.5 h, 2 h and 4 h at 37 °C and 5% CO_2. Untreated trypanosome cells (1 mL) were harvested as control (0 h). Harvested cells (1 mL) were centrifuged for 1 min at 3000 x g, washed with PBS, and the pellet was re-suspended in 50 µL of PBS. The same volume of 7.2% formaldehyde (in PBS) was added and the cells were

fixed for 30 minutes. Then, cells were centrifuged for 1 min at 3000 x g, the pellet was re-suspended in 100 µL of PBS and 50 µL were pipetted on a poly-lysine-coated glass microscope slide. In order to achieve attachment of the cells to the slide, cells were incubated for 15 min in a humid chamber. Afterwards, the cells were carefully washed with PBS and additionally fixed with ice-cold methanol for at least 30 min. Then, cells were washed with PBS, stained with 150 µL DAPI (1 µg/mL) for 5 min, washed again with PBS and finally washed with distilled water. Vectashield Mounting Medium (5 µL, Vector Laboratories) was added, and a cover slip was placed on top. Images were taken using the DAPI filter set and differential interference contrast (DIC) on a Zeiss Axioplan microscope equipped with a SPOT Pursuit CCD camera (Diagnostic Instruments) and Visiview software (Visitron, Germany).

2.2.4. Porcine microtubules sedimentation assay and SDS-PAGE

The sedimentation assay with porcine tubulin was carried out in order to show direct effects of the test compounds on tubulin [48,49]. 100 µL tubulin (1 mg/mL purified pig brain tubulin in Brinkley BR buffer BRB80), DTT and GTP (1 mM) were added to start tubulin polymerisation. Taxol was added in 3 steps; at first 10 µM was added and incubated for 5 min at 37 °C, then 100 µM was added and incubated for 5 min at 37 °C, and finally 1 mM was added and incubated for 15 min. The stabilised tubulin samples were centrifuged for 15 min at 250000 x g at 30 °C. Meanwhile, PME (polymerisation buffer, 2 mL: 80 mM PIPES, 2 mM $MgCl_2$, 0.5 mM EGTA, 1 mM DTT, 1 mM GTP and 10 µM taxol) was prepared. After centrifugation, the supernatant was discarded and the pellet carefully suspended in the PME buffer. The microtubule samples were treated with the test compounds (1 µM, 2.5 µM, 5 µM, 10 µM) and incubated for 30 min, 1 h, or 2 h at 37 °C. The samples were centrifuged at 250000 x g and 23 °C for 10 min. The supernatant was taken and stored on ice and the pellet was suspended in PME with 5 mM $CaCl_2$ and 50 mM KCl and stored on ice. Samples were treated with hot Laemmli

buffer, incubated for 10 min at 95 °C, and separated on a 10% SDS-PAGE gel. The gels were stained with Coomassie solution (0.25% Coomassie Brilliant Blue R250, 10% acetic acid, 50% methanol) and destained in 10% acetic acid, 40% methanol. Gels were scanned and the tubulin bands were densitometrically analysed by *ImageJ*.

2.2.5. *T. b. brucei microtubules sedimentation assay, SDS-PAGE and western blot*

Trypanosome cells ($1.3x10^6$/mL) were placed in 6-well plates and incubated with the test compounds **1a** or **1b** (1 µM). Cells were harvested at 0 h, 0.5 h, 2 h and 4 h, centrifuged for 2 min at 2000 x g, and washed with PBS. The pellet was re-suspended in 0.5% NP40/PEME (50 µL). The cells were incubated on ice for 5 min, centrifuged for 1 min at 3000 x g and the supernatant was placed in a new Eppendorf tube. Hot 2x Laemmli buffer (50 µL) was added to the supernatant and hot 1x Laemmli buffer (100 µL) to the pellet followed by incubation at 95 °C for 10 min. SDS-polyacrylamide gels, Coomassie staining and Western blotting were done following standard methods.

Antibodies: A mouse monoclonal antibody against the *T. brucei* homologue of luminal ER protein BiP (GeneDB identifier Tb927.11.7460) was prepared by immunizing BALB/cByJ mice (Janvier Labs, France) with an affinity-purified, full-length recombinant His6-BiP protein, produced in *E. coli*. Spleen lymphocytes were fused with P3X63-Ag8.653 myeloma cells and hybridomas selected using HAT-containing OptiMEM-medium with 10% FCS (Thermo Fisher Scientific). Primary screening was carried out by ELISA and positive clones were re-tested by Western-blotting and immunofluorescence. The resulting hybridoma cell line produced a highly specific (by Western blot and immunofluorescence) anti-BiP IgG1. The anti-beta-tubulin mouse monoclonal antibody TAT1 was a kind gift of Keith Gull (University of Oxford).

3. Results and discussion

3.1. Trypanocidal activity of gold complexes

Gold(I) complexes **1a** and **1b** were prepared according to literature procedures and tested for their trypanocidal activity against *T. b. brucei* parasites by the Alamar Blue (AB) assay (Table 1) [41,42]. Both gold complexes exhibited excellent activity against *T. b. brucei* cells with IC_{50} values in the low nanomolar or sub-nanomolar range. The gold complexes **1a** and **1b** showed stronger activity than the well-known tubulin binders colchicine (IC_{50} = 1.4 µM) and vinblastine (IC_{50} = 0.1 µM) as reported elsewhere [17]. In addition, the complexes **1a** and **1b** were distinctly less toxic to human HeLa cells and displayed lower growth inhibitory activity when compared with treated *T. b. brucei* cells (Table 1). The *T. b. brucei* selectivity index (SI) is a marker for the clinical applicability of new anti-trypanosomal compounds (the greater the SI, the more selective is the new drug candidate). Pentamidine as a clinically approved drug against *T. brucei* infections showed the best SI value. Nevertheless, complexes **1a** and **1b** exhibited SI values of 77 and 148, respectively (Table 1) and, thus, these compounds may be suitable for further *in vivo* testing of *T. brucei* models in laboratory animals.

Table 1. Inhibitory concentrations IC_{50} (72 h) [nM] of compounds **1a**, **1b**, and pentamidine from AB assays against cells of *T. b. brucei* and human HeLa cells (mean of three values, standard deviation < ±15%) and *T. b. brucei* selectivity index (SI), IC_{50}(HeLa cells)/IC_{50}(*T. b. brucei* cells) of compounds **1a**, **1b**, and pentamidine.

Compd.	*T. b. brucei*	HeLa	SI
1a	3.01	231	77
1b	0.93	138	148
Pentamidine	0.042	1470	35000

3.2. Effects of gold complexes on the T. b. brucei cytoskeleton

T. b. brucei cells were treated with the gold complexes **1a** and **1b** and their effects on the cytoskeleton were analysed via fluorescence microscopy. At first, the effects of complex **1a** (0.1 µM, 1 µM, 10 µM) were investigated (Fig. 2, Fig. S2, Fig. S3). The

obtained results were compared with untreated *T. b. brucei* cells (Fig. 2, Fig. S1, see supplementary data).

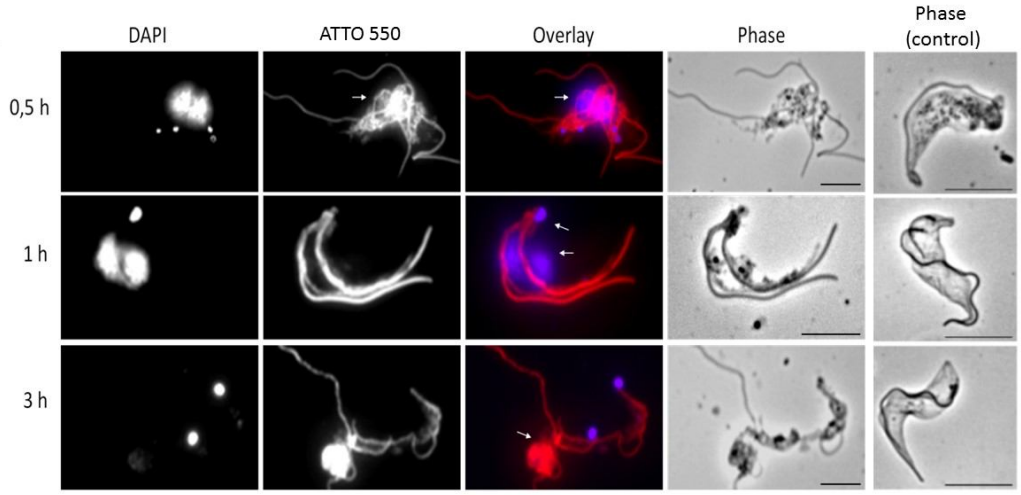

Fig. 2. Immunofluorescence images of MeOH-fixed *T. b. brucei* cells after incubation with **1a** (1 µM) for 0.5 h, 1 h, and 3 h (bar = 10 µm). Signals of DAPI (DNA), ATTO 550 (tubulin), the overlay of both and the phase contrast as well as the phase contrast of untreated cells (phase control, bar = 15 µm) are shown. Arrows mark the microtubule fragments (red in the overlay) and changes in the nucleus and kinetoplast (blue in the overlay).
((2-column fitting image))

At concentrations of 1 µM and 10 µM, gold complex **1a** caused a complete disintegration of the cytoskeleton already after 0.5 h incubation time. Cell debris consisting of remnants of the cytoskeleton and nucleus as well as intact flagellum components were observed. The microtubules of the flagellum appear to be resistant to attacks by the gold complex. In order to rule out any deceptive effects of the NP40 fixing agent, the experiment was repeated for **1a**-treated cells without NP40 fixation and showed similar effects (Fig. 3). Significant cell rounding was fully expressed already after 2 h while after 4 h the treated cells disintegrated. In addition, light microscopic investigations of intact parasite cells treated with **1a** (10 µM) revealed reduced motility of parasite cells already after 20 min.

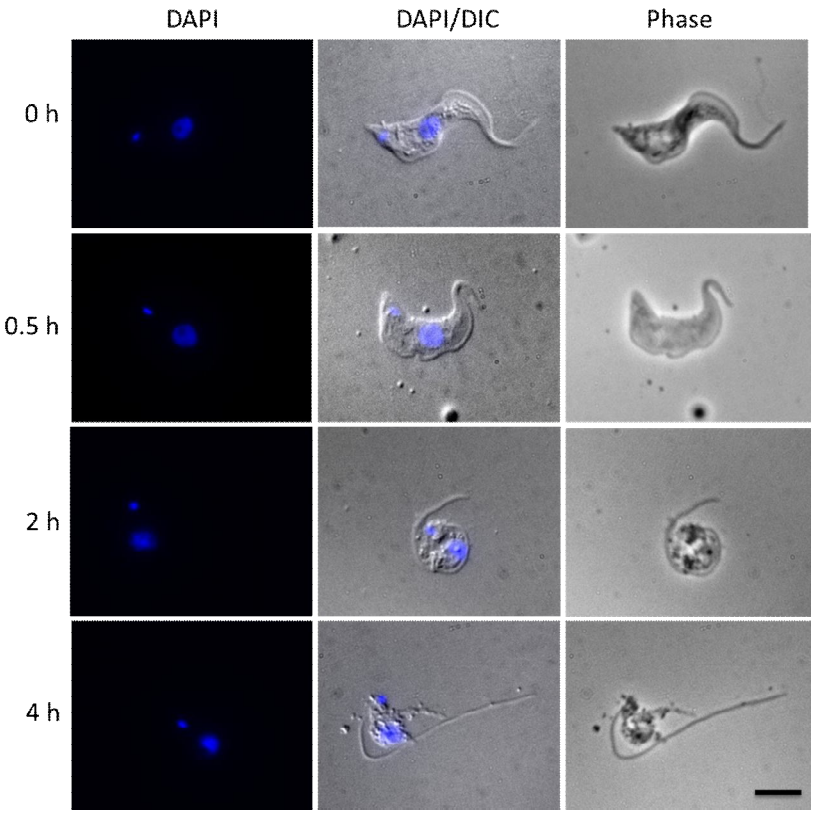

Fig. 3. Immunofluorescence images of MeOH-fixed *T. b. brucei* cells after incubation with **1a** (1 µM) for 0.5 h, 2 h, and 4 h when compared with untreated control cells (0 h; bar = 5 µm). Signals of DAPI (DNA, blue) and the phase contrast are shown. ((1.5-column fitting image))

Human HeLa cells were treated with **1a** in the same way to the *T. b. brucei* cells and the morphological changes were analysed (Fig. 4) in comparison with untreated HeLa cells (Fig. S4, see supplementary data). Already 1 h after incubation with **1a** (10 µM) the microtubule network showed signs of disintegration. An accumulation of tubulin was observed near the cell membrane. However, a complete destruction and separation of the tubulin scaffold was not observed. In addition, DAPI signals of the nucleus indicated no morphological changes in contrast to the *T. b. brucei* cells. At lower dose of **1a** (1 µM), the cell structure remained intact. Only after incubation for 6 h, anomalies of the cytoskeletal structure became visible (Fig. S5, see supplementary data).

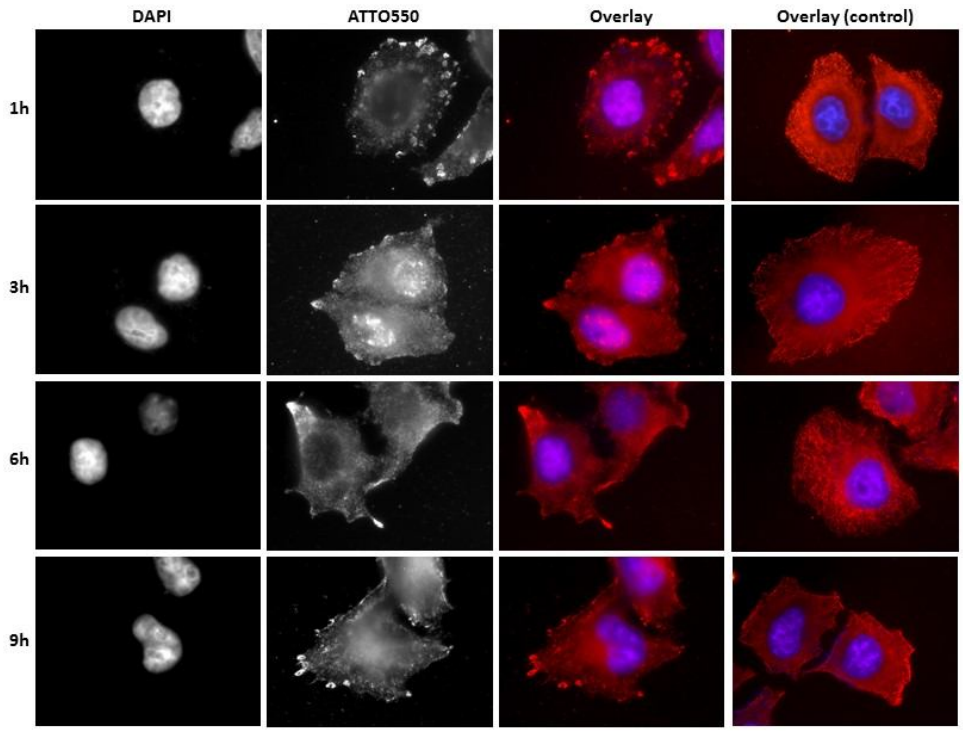

277

278 **Fig. 4.** Immunofluorescence images of MeOH-fixed HeLa cells after incubation with **1a**
279 (10 µM) for 1 h, 3 h, 6 h, and 9 h (bar = 50 µm). Signals of DAPI (DNA), ATTO 550
280 (tubulin), the overlay of both and the overlay of untreated HeLa cells (overlay control)
281 are shown. ((2-column fitting image))

282 Then, the effects of the ferrocene-gold complex **1b** on the morphology of *T. b.*
283 *brucei* cells were investigated in detail. At a dose of 10 µM dead cells were observed
284 already after 0.5 h (Fig. S6, see supplementary data). After longer incubation times the
285 parasite cells were completely destroyed and the sub-pellicular microtubules no longer
286 detectable. However, DAPI signals of the nucleus as well as apparently intact flagellum
287 components were visible. Deformation of the nucleus and of the tubulin network was
288 observed at a lower dose of 1 µM. In some cases, the flagellum was separated from the
289 cell body (Fig. 5). Dying parasite cells were visible with much cell debris at 0.1 µM as
290 well (Fig. S7, see supplementary data). Light microscopic investigations showed that

after treatment with **1b** (10 µM) for 20-25 min intact parasite cells were less motile than untreated control cells.

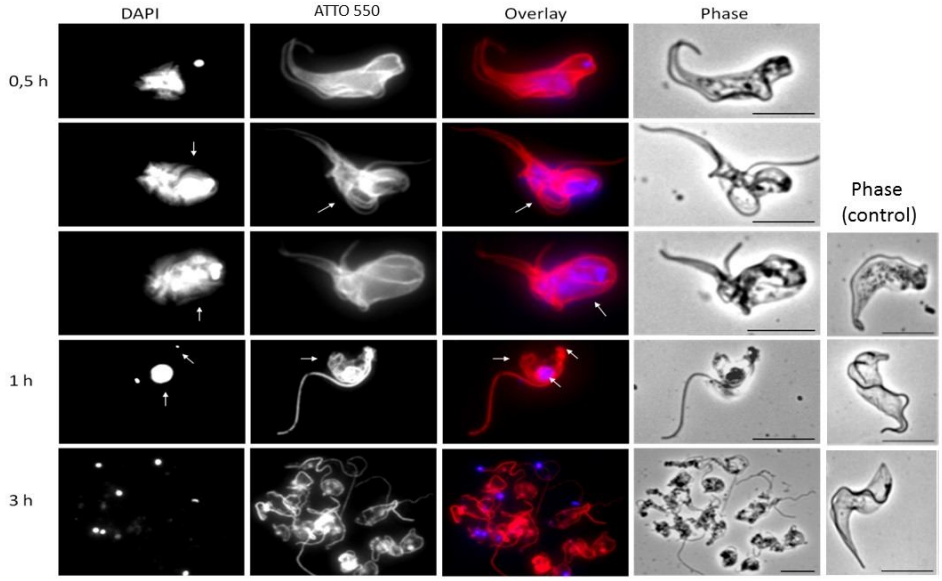

Fig. 5. Immunofluorescence images of MeOH-fixed *T. b. brucei* cells after incubation with **1b** (1 µM) for 0.5 h (top three lanes), 1 h, and 3 h (bar = 10 µm). Signals of DAPI (DNA), ATTO 550 (tubulin), the overlay of both, the phase contrast as well as the phase contrast of untreated cells (phase control, after 0.5 h, 1 h, 3 h, bar = 15 µM) are shown. Arrows mark cytoskeletal anomalies (red in the overlay) and changes of the nucleus and kinetoplast regions (blue in the overlay). ((2-column fitting image))

Again, in order to exclude any deceptive effects of NP40, images of cells fixed without NP40 were investigated (Fig. 6). Like in the case of **1a**, cell rounding occurred already 2 h after treatment with **1b** and cell disintegration started after 4 h. Already after 0.5 h, the morphology of the treated *T. b. brucei* cells started to change.

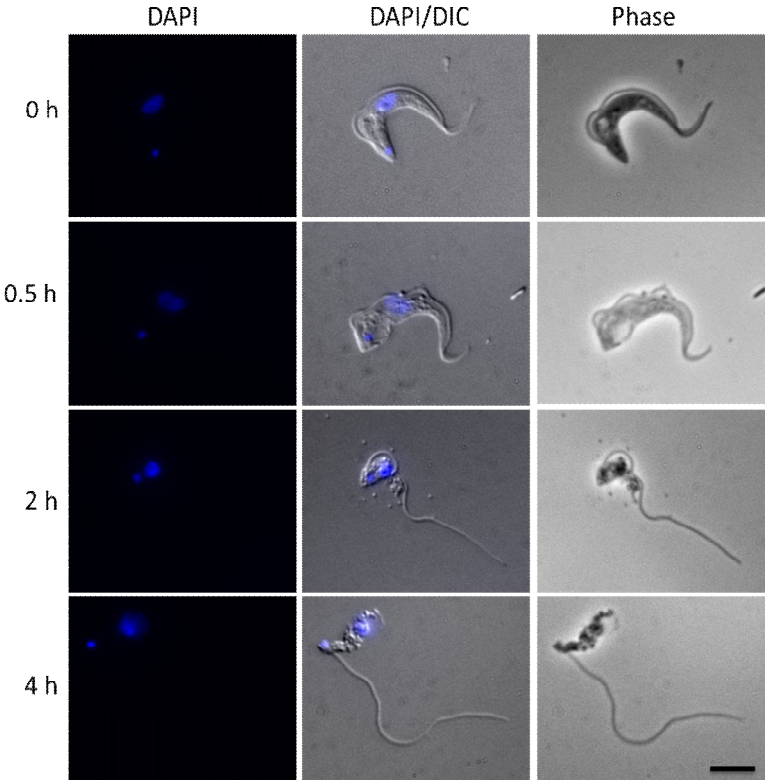

Fig. 6. Immunofluorescence images of MeOH-fixed *T. b. brucei* cells after incubation with **1b** (1 µM) for 0.5 h, 2 h, and 4 h when compared with untreated control cells (0 h; bar = 5 µm). Signals of DAPI (DNA, blue) and the phase contrast are shown.
((1.5-column fitting image))

In human HeLa cells, complex **1b** (10 µM) caused no changes in the cell morphology after short incubation times of 1 h and 3 h (Fig. 7). Only after 6 h changes in the microtubule scaffold were observed as well as accumulation of tubulin near the membrane. In contrast to the *T. b. brucei* cells, the microtubule scaffold of the HeLa cells was not completely destroyed. No changes of the HeLa cell nucleus were observed either. At lower dose of **1b** (1 µM) no distinct morphological changes of the cytoskeleton and the nucleus of the HeLa cells could be observed (Fig. S8, see supplementary data).

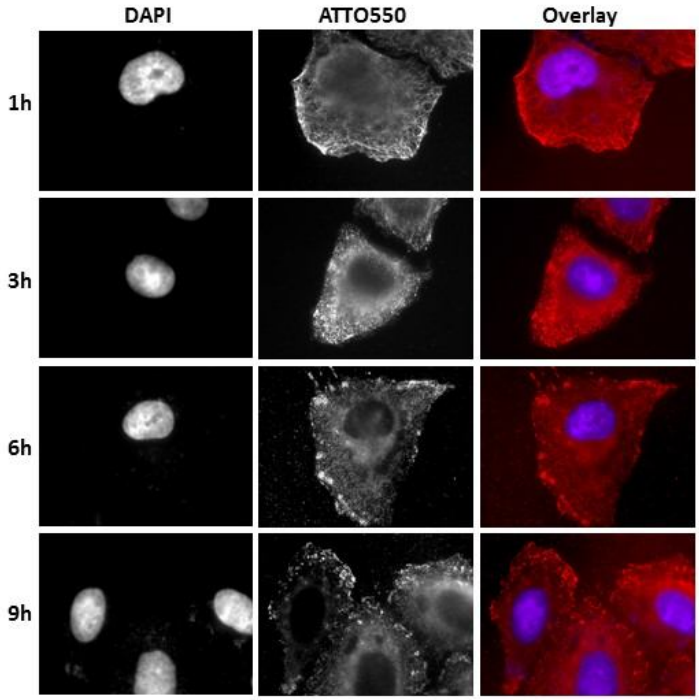

317

318 **Fig. 7.** Immunofluorescence images of MeOH-fixed HeLa cells after incubation with **1b**
319 (10 µM) for 1 h, 3 h, 6 h, and 9 h (bar = 50 µm). Signals of DAPI (DNA), ATTO 550
320 (tubulin), and the overlay of both. Untreated cells (overlay control) of this experiment
321 are shown in Fig. 4. ((one-column fitting image))

322 In contrast to the observed microtubule damages induced by **1a** and **1b** in *T. b. brucei*
323 cells, both compounds **1a** and **1b** have displayed damage of actin cytoskeleton and
324 induced vascular disruption of blood vessels in certain cancer cell lines [41,42].
325 Consequently, both gold(I) complexes **1a** (15 mg/kg, i.p.) and **1b** (7.5 mg/kg, i.p.) were
326 also active *in vivo* against highly metastatic B16-F10 mouse melanoma xenografts
327 without side effects (i.e., weight reduction) at the given doses [41,42]. Due to the
328 distinctly higher *in vitro* activities of **1a** and **1b** against *T. b. brucei* cells when
329 compared with human cells (including cancer cells), it is likely that much lower doses
330 than 7.5 or 15 mg/kg for future *in vivo* experiments in animals with suitable *T. brucei*
331 models will be sufficient for efficient treatment of sleeping sickness. It is conceivable

that reduced active doses of the complexes will be more tolerable or less toxic to the animal which makes these compounds very suitable drug candidates for advanced *in vivo* testing against *T. brucei* models.

3.3. Effects of gold complexes on tubulin polymerisation

The effects of the gold complexes **1a** and **1b** on the polymerisation of porcine tubulin were investigated by a sedimentation assay (Fig. S9, Fig. S10, see supplementary data). The fractions of polymerised microtubules (pellet fraction) versus depolymerised tubulin (supernatant fraction) after treatment with the complexes followed by ultracentrifugation were determined via separation of both fractions on SDS-PAGE gels. Only **1b** inhibited tubulin polymerisation (52% of depolymerised tubulin) at the highest dose (10 µM) after 2 h of incubation (Fig. S9). At a lower dose of 1 µM complex **1b** exhibited distinctly reduced tubulin depolymerisation (15% of depolymerised tubulin). No effect was observed after a shorter incubation time (1 h, Fig. S10) either. In addition, the effects of compounds **1a** and **1b** on *T. b. brucei* microtubules was investigated. Sedimentation assay followed by Coomassie staining revealed only general protein degradation during the course of drug treatment (Fig. S11). Similarly, western blot analysis of cellular tubulin from treated *T. b. brucei* cells showed a general reduction of protein (both of tubulin/microtubules and of the BIP marker) in a time-dependent manner indicating general reduction of protein levels in the dying *T. b. brucei* cells (Fig. 8). Thus, depolymerisation of microtubules is unlikely the main mode of action of the complexes **1a** and **1b**, and the noteworthy cytoskeleton damaging effect of these gold compounds must have different and rather indirect reasons.

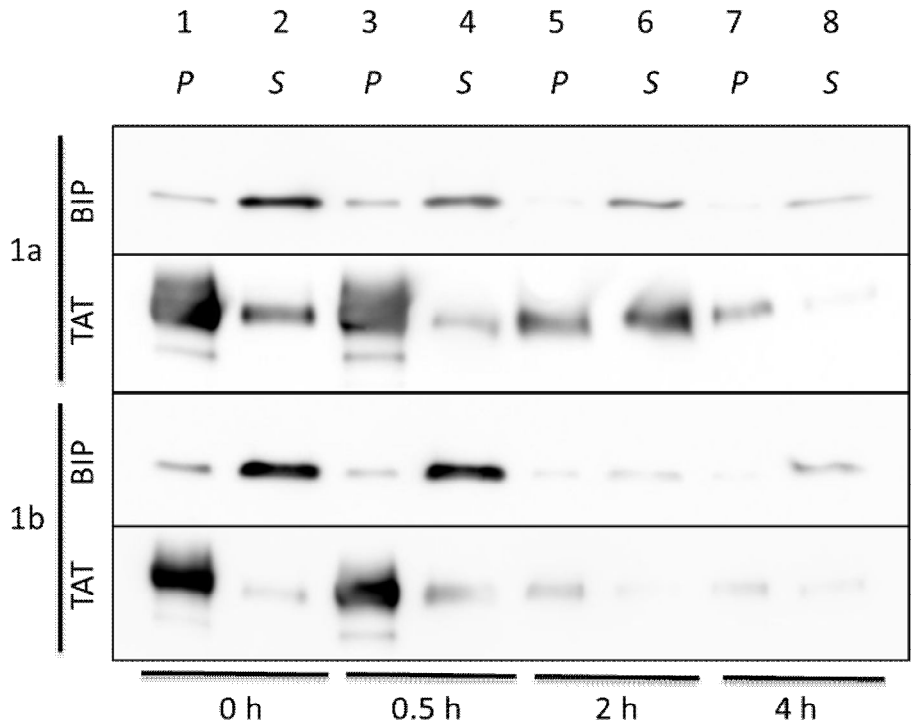

355

356 **Fig. 8.** Soluble and insoluble fractions of lysates from *T. b. brucei* cells treated with
357 compounds **1a** or **1b** (1 µM) for the indicated time points and visualized by Western
358 blot using anti-tubulin antibody and anti-BiP (marker for soluble protein located in the
359 lumen of the endoplasmic reticulum). Lanes 1, 3, 5, 7: pellet; lanes 2, 4, 6, 8:
360 supernatant. P = pellet fraction; S = supernatant fraction. ((1.5-column fitting image))

361 **4. Conclusions**

362 The cationic gold(I) NHC-complexes **1a** and **1b** exhibited excellent trypanocidal
363 activity in the low nanomolar and sub-nanomolar range. Their mode of action appears to
364 involve severe cytoskeleton destruction after short incubation times and at low doses.
365 This damage differs from the damage induced in human HeLa cells. In the case of **1b**,
366 the damage in the human cells was limited, neither cytoskeleton destruction nor changes
367 of the nucleus were observed. Together with the results obtained from AB assays with
368 human HeLa cells, a significant selectivity for trypanosomes was observed for the gold
369 complexes, in particular, for the ferrocene conjugate **1b**. An inhibition of tubulin
370 polymerisation or a destabilisation of intact microtubules can be a mode of action for

371 complex **1b** at high doses only. Hence, further investigations to elucidate other targets
372 of these interesting gold complexes are necessary. Proteins of the parasitic spindle
373 apparatus and factors involved in the formation and regulation of the *T. brucei*
374 cytoskeleton such as kinesins may be conceivable targets for the complexes **1a** and **1b**.
375 Due to the quick onset of the cytoskeleton damage in the *T. b. brucei* cells efficient drug
376 uptake mechanisms may play a role for the strong activity of **1a** and **1b** in these
377 parasitic cells as well.
378

379 **Acknowledgments**

380 We thank the Deutsche Forschungsgemeinschaft for financial support (grant Scho
381 402/12-1) and Keith Gull, University of Oxford, for kindly providing the TAT antibody.
382

383 **Supplementary data**

384 Supplementary data associated with this article (additional immunofluorescence
385 images Fig. S1-S8, SDS-PAGE gel images Fig. S9-S11, and graphs of the Alamar Blue
386 assays Fig. S12-S17) can be found, in the online version, at
387 doi:10.1016/j.molbiopara.2017.00.000.

388

389 **References**

390 [1] P. MacGregor, K.R. Matthews, New discoveries in the transmission biology of
391 sleeping sickness parasites: applying the basics, J. Mol. Med. 88 (2010) 865-871.

392 [2] R. Lucius, B. Loos-Frank. Parasitologie: Grundlagen für Biologen, Mediziner und
393 Veterinärmediziner. Heidelberg: Spektrum Akad. Verlag; 1997.

394 [3] D.H. Smith, J. Pepin, A.H.R. Stich, Human African trypanosomiasis: an emerging
395 public health crisis, Br. Med. Bull. 54 (1998) 341-355.

396 [4] J. Pépin, H.A. Méda, The epidemiology and control of human African
397 trypanosomiasis, Adv. Parasitol. 49 (2001) 71-132.

398 [5] D.A. Maslov, S.A. Podlipaev, J. Lukes, Phylogeny of the kinetoplastida:
399 taxonomic problems and insights into the evolution of parasitism, Mem. Inst.
400 Oswaldo Cruz 96 (2001) 397-402.

401 [6] M.P. Barrett, A.H. Fairlamb, The biochemical basis of arsenical-diamidine
402 crossresistance in African trypanosomes, Parasitol. Today 15 (1999) 136-140.

403 [7] M.P. Barrett, The fall and rise of sleeping sickness, Lancet 353 (1999) 1113-1114.

404 [8] M.A.J. Ferguson, A.K. Allen, D. Snary, The detection of phosphonolipids in the
405 protozoan *Trypanosoma cruzi*, Biochem. J. 207 (1982) 171-174.

406 [9] J.D. Barry, The relative significance of mechanisms of antigenic variation in
407 African trypanosomes, Parasitol. Today 13 (1997) 212-218.

408 [10] K.R. Matthews, J.R. Ellis, A. Paterou, Molecular regulation of the life cycle of
409 African trypanosomes, Trends Parasitol. 20 (2004) 40-47.

410 [11] D. Steverding, The history of African trypanosomiasis, Parasit. Vectors 1 (2008)
411 3.

412 [12] M.P. Barrett, D.W. Boykin, R. Brun, R.R. Tidwel, Human African
413 trypanosomiasis: pharmacological re-engagement with a neglected disease, Br. J.
414 Pharmacol. 152 (2007) 1155-1171.

415 [13] T.N. Baral, Immunobiology of African trypanosomes: need of alternative
416 interventions, J. Biomed. Biotech. 2010 (2010) 389153.

417 [14] M. Schlitzer, Wirkstoffe zur Behandlung der Afrikanischen Schlafkrankheit,
418 Pharm. Unserer Zeit 38 (2009) 552-558.

419 [15] K.R. Matthews, 25 years of African trypanosome research: from description to
420 molecular dissection and new drug discovery, Mol. Biochem. Parasitol. 200 (2015)
421 30-40.

422 [16] M.M. Chan, D. Fong, Plant microtubule inhibitors against trypanosomatids,
423 Parasitol. Today 10 (1994) 448-451.

424 [17] D.O.K. Ochola, R.K. Prichard, G.W. Lubega, Classical ligands bind tubulin of
425 trypanosomes and inhibit their growth *in vitro*, J. Parasitol. 88 (2002) 600-604.

426 [18] V. Nanavaty, R. Lama, R. Sandhu, B. Zhong, D. Kulman, V. Bobba, A. Zhao, B.
427 Li, B. Su, Orally active and selective tubulin inhibitors as anti-trypanosome agents,
428 PLoS ONE 11 (2016) e0146289.

429 [19] K.Y. Chan, K. Ersfeld, The role of the Kinesin-13 family protein TbKif13-2 in
430 flagellar length control of *Trypanosoma brucei*, Mol. Biochem. Parasitol. 174
431 (2010) 137-140.

432 [20] K.Y. Chan, K.R. Matthews, K. Ersfeld, Functional characterization and drug
433 target validation of a mitotic Kinesin-13 in *Trypanosoma brucei*, PLoS Pathog. 6
434 (2010) e1001050.

435 [21] C.E. Walczak, S. Gayek, R. Ohi, Microtubule-depolymerizing kinesins, Annu.
436 Rev. Cell Dev. Biol. 29 (2013) 417-441.

437 [22] S.P. Fricker, Medical uses of gold compounds: past, present and future, Gold Bull.
438 29 (1996) 53-60.

439 [23] C.F. Shaw III, Gold-based therapeutic agents, Chem. Rev. 99 (1999) 2589-2600.

[24] B. Biersack, A. Ahmad, F.H. Sarkar, R. Schobert, Coinage metal complexes against breast cancer, Curr. Med. Chem. 19 (2012) 3949-3956.

[25] M. Navarro, Gold complexes as potential anti-parasitic agents, Coord. Chem. Rev. 253 (2009) 1619-1626.

[26] A. Ilari, P. Baiocco, L. Messori, A. Fiorillo, A. Boffi, M. Gramiccia, T. di Muccio, G. Colotti, A gold-containing drug against parasitic polyamine metabolism: the X-ray structure of trypanothione reductase from *Leishmania infantum* in complex with auranofin reveals a dual mechanism of enzyme inhibition, Amino Acids 42 (2012) 803-811.

[27] C. Hemmert, A. Fabié, A. Fabre, F. Benoit-Vical, H. Gornitzka, Synthesis, structures, and antimalarial activities of some silver(I), gold(I) and gold(III) complexes involving N-heterocyclic carbene ligands, Eur. J. Med. Chem. 60 (2013) 64-75.

[28] P.V. Simpson, C. Schmidt, I. Ott, H. Bruhn, U. Schatzschneider, Cellular uptake and biological activity against pathogenic microorganisms and cancer cells of rhodium and iridium N-heterocyclic carbene complexes bearing charged substituents, Eur. J. Inorg. Chem. (2013) 5547-5554.

[29] C. Ornelas, Application of ferrocene and its derivatives in cancer research, New J. Chem. 35 (2011) 1973-1985.

[30] E. Meléndez, Metallocenes as target soecific drugs for cancer treatment, Inorg. Chim. Acta 393 (2012) 36-52.

[31] S.S. Braga, A.M.S. Silva, A new age for iron: antitumoral ferrocenes, Organometallics 32 (2013) 5626-5639.

463 [32] R. Schobert, S. Knauer, S. Seibt, B. Biersack, Anticancer active illudins: recent
464 developments of a potent alkylating compound class, Curr. Med. Chem. 18 (2011)
465 790-807.

466 [33] S. Knauer, B. Biersack, M. Zoldakova, K. Effenberger, W. Milius, R. Schobert,
467 Melanoma-specific ferrocene esters of the fungal cytotoxin illudin M, Anti-Cancer
468 Drugs 20 (2009) 676-681.

469 [34] R. Schobert, S. Seibt, K. Mahal, A. Ahmad, B. Biersack, K. Effenberger-
470 Neidnicht, S. Padhye, F.H. Sarkar, T. Mueller, Cancer selective
471 metallocenedicarboxylates of the fungal cytotoxin illudin M, J. Med. Chem. 54
472 (2011) 6177-6182.

473 [35] C. Spoerlein-Guettler, K. Mahal, R. Schobert, B. Biersack, Ferrocene and
474 (arene)ruthenium(II) complexes of the natural anticancer naphthoquinone
475 plumbagin with enhanced efficacy against resistant cancer cells and a genuine mode
476 of action, J. Inorg. Biochem. 138 (2014) 64-72.

477 [36] A. Ahmad, K. Mahal, S. Padhye, F.H. Sarkar, R. Schobert, B. Biersack, New
478 ferrocene modified lawsone Mannich bases with anti-proliferative activity against
479 tumor cells, J. Saudi Chem. Soc. 21 (2017) 105-110.

480 [37] J.K. Muenzner, A. Ahmad, M. Rothemund, S. Schrüfer, S. Padhye, F.H. Sarkar,
481 R. Schobert, B. Biersack, Ferrocene-substituted 3,3'-diindiolylmethanes with
482 improved anticancer activity, Appl. Organometal. Chem. 30 (2016) 441-445.

483 [38] A. Baramee, A. Coppin, M. Mortuaire, L. Pelinski, S. Tomavo, J. Brocard,
484 Synthesis and in vitro activities of ferrocenic aminohydroxynaphthoquinones
485 against *Toxoplasma gondii* and *Plasmodium falciparum*, Bioorg. Med. Chem. 14
486 (2006) 1294-1302.

487 [39] F. Dubar, J. Khalife, J. Brocard, D. Dive, C. Bioth, Ferroquine, an ingenious
488 antimalarial drug – thoughts on the mechanism of action, Molecules 13 (2008)
489 2900-2907.

490 [40] A.M.A. Velásquez, A.I. Francisco, A.A.N. Kohatsu, F.A. de Jesus Silva, D.F.
491 Rodrigues, R.G. da Silva Teixeira, B.G. Chiari, M.G.J. de Almeida, V.L.B. Isaac,
492 M.D. Vargas, R.M.B. Cicarelli, Synthesis and tripanocidal activity of ferrocenyl and
493 benzyl diamines against *Trypanosoma brucei* and *Trypanosoma cruzi*, Bioorg. Med.
494 Chem. Lett. 24 (2014) 1707-1710.

495 [41] J.K. Muenzner, B. Biersack, H. Kalie, I.C. Andronache, L. Kaps, D. Schuppan, F.
496 Sasse, R. Schobert, Gold(I) biscarbene complexes derived from vascular-disrupting
497 combretastatin A-4 address different targets and show antimetastatic potential,
498 ChemMedChem 9 (2014) 1195-1204.

499 [42] J.K. Muenzner, B. Biersack, A. Albrecht, T. Rehm, U. Lacher, W. Milius, A.
500 Casini, J.-J. Zhang, I. Ott, V. Brabec, O. Stuchlikova, I.C. Andronache, L. Kaps, D.
501 Schuppan, R. Schobert, Ferrocenyl-coupled N-heterocyclic carbene complexes of
502 gold(I): a successful approach to multinuclear anticancer drugs, Chem. Eur. J. 22
503 (2016) 18953-18962.

504 [43] E. Wirtz, S. Leal, C. Ochatt, G.A. Cross, A tightly regulated inducible expression
505 system for conditional gene knock-outs and dominant-negative genetics in
506 *Trypanosoma brucei*, Mol. Biochem. Parasitol. 99 (1999) 89-101.

507 [44] R.S. Twigg, Oxidation-reduction aspects of resazurin, Nature 155 (1945) 401-402.

508 [45] R.D. Fields, M.V. Lancaster, Dual-attribute continuous monitoring of cell
509 proliferation/cytotoxicity, Am. Biotechnol. Lab. 11 (1993) 48-50.

510 [46] S.A. Ahmed, R.M. Gogal Jr, J.E. Walsh, A new rapid and simple non-radioactive
511 assay to monitor and determine the proliferation of lymphocytes: an alternative to
512 [3H]thymidine incorporation assay, J. Immunol. Methods 170 (1994) 211-224.

513 [47] S. Al-Nasiry, N. Geusens, M. Hanssens, C. Luyten, R. Pijnenborg, The use of
514 Alamar Blue assay for quantitative analysis of viability, migration and invasion of
515 choriocarcinoma cells, Hum. Rep. 22 (2007) 1304-1309.

516 [48] A. Desai, C.E. Walczak, Assays for Microtubule-destabilizing kinesins, Mol.
517 Biol. 164 (2001) 109-121.

518 [49] L.Y. Hung, H.-L. Chen, C.-W. Chang, B.-R. Li, T.K. Tang, Identification of a
519 novel microtubule-destabilizing motif in CPAP that binds to tubulin heterodimers
520 and inhibits microtubule assembly, Mol. Biol. Cell. 15 (2004) 2697-2706.